DOW RADAR OBSERVATIONS OF WIND FARMS

BY MALLIE TOTH, ERIN JONES, DUSTIN PITTMAN, AND DAVID SOLOMON

Mobile radar observations provide insight into the types of interference that can be expected in WSR-88D and local television radar operations as wind farms expand to locations closer to operational radars.

The growth of the alternative energy industry in the United States in recent years has led to an increasing number of wind farms nationwide. In 2008, the Department of Energy announced plans for the country to meet 20% of its energy needs through wind power by 2030 (U.S. Department of Energy 2008); to meet this quota, an estimated 50,000 km^2 of land and ocean will have to be utilized. Although the bulk of the new turbines are expected to be placed offshore, continental-based wind farms will occupy an area estimated to be about the size of Rhode Island. The expansion of wind farms has already proven to be problematic for the meteorological community, because turbines can interfere with Doppler weather radar observations. The nationwide Weather Surveillance Radar-1988 Doppler (WSR-88D) network provides coverage to nearly the entire continental United States at the level of ~10,000 ft (~3000 m) (Crum and Alberty 1993), which means that almost all land-based wind farms will be within some range of a WSR-88D, though many WSR-88Ds may still overshoot wind farms. Wind turbines already built within close enough range of these radars, however, have resulted in ▶

DOW7 at the Montezuma Wind Farm outside of Dodge City, KS during the 2010 season of the VORTEX2 project. Photo by Erin Jones.

false returns in all three moments of the Doppler spectrum: reflectivity, velocity, and spectrum width (Crum et al. 2008). The farms are not filtered out as ground clutter, which is assumed to be stationary, because working turbines have velocity signatures associated with them (Vogt et al. 2007). The return from turbine blades has resulted in both the appearance of extremely high (>70 dBZ) radar reflectivity factor (hereafter referred to as reflectivity) values and the detection of false mesocyclones by WSR-88D algorithms (e.g. Burgess et al. 2007; Vogt et al. 2007). Additionally, because the wind turbine clutter (WTC) is not filtered out automatically, derived products like precipitation estimates are also contaminated (Crum 2010).

Two WSR-88D locations, in particular, have been used in numerous studies of the impact of the turbine clutter on Doppler radar operations (e.g., Burgess et al. 2007; Isom et al. 2009; Vogt et al. 2007; Hood et al. 2010). The Dodge City, Kansas (KDDC), and Great Falls, Montana (KTFX), WSR-88Ds have experienced interference from wind farms located within range of their sites. Data collection at the KTFX site, which is 6 km away from a single wind farm, has been impacted by multipath scattering and multitrip false echoes, and Doppler radar measurements at KDDC, which has two wind farms within its operational range, have been contaminated by the false detection of tornadoes from WSR-88D algorithms, among other things (Isom et al. 2009; Vogt et al. 2007). Additional problems elsewhere in the country may stem from the placement of wind turbines on elevated ground, which would enhance the amount of wind received by the turbine but consequently create interference with the radar at ranges that might otherwise be too distant.

WSR-88D mesocyclone detection algorithms and tornado detection algorithms identify potential vortices by evaluating the velocity field and applying specific data thresholds (Stumpf et al. 1998; Mitchell et al. 1998). The algorithms search for azimuthal shear in adjacent beams and apply minimum strength and aspect ratio thresholds to the data to eliminate weak or outlying segments. Thresholds are applied in both the reflectivity and radial velocity fields. Although only the mesocyclone detection algorithm requires a time association, both employ a depth criterion for detection: 3 km for mesocyclone detection and 1.5 km for tornado detection. The mesocyclone algorithm has been triggered by WTC observed by WSR-88Ds, and there is currently no automated method available to remove this interference (Vogt et al. 2007).

Attempts to mitigate the effects wind farms have on Doppler radars have mostly been successful in removing the signatures created by stationary turbines, which are filtered out like ground clutter. Contamination from moving blades, however, is difficult to remove without also removing the characteristics of the weather occurring in the immediate surrounding environment (Isom et al. 2009). Automated removal of WTC is important for the proper detection of features as well as for the proper application of derived products, like precipitation estimation (Crum 2010). Although research on WTC mitigation is still in its early stages for WSR-88D operations, wind farms are likely to impact radar observations made by other platforms, such as the Collaborative Adaptive Sensing of the Atmosphere (CASA) network of small, relatively low-cost radars (see Brotzge et al. 2006; McLaughlin et al. 2009). This dense network of radars examines phenomena in the lowest 3 km of the atmosphere, the primary region experiencing interference from wind farms. Furthermore, nonmeteorological radars such as those used for air traffic control have also encountered mitigation issues with the advent of wind farms (Perry and Biss 2007).

This study uses a mobile Doppler radar to examine wind turbine clutter on a small scale within close proximity to wind turbines (less than 1 km). These radar observations are compared to the radar observations of a local television station and the closest WSR-88D. Data from a clear-air day and a day with intense rainfall and strong winds show a range of environmental and operating conditions in which wind turbines can create interference.

BACKGROUND. The Doppler on Wheels (DOW) is a mobile 3-cm-wavelength Doppler radar with a ~1° beamwidth. It was developed for the collection of high-resolution Doppler radar data at close range to meteorological phenomena such as tornadoes and their associated parent storms, hurricanes, and

AFFILIATIONS: Toth, Jones, Pittman, and Solomon—Department of Earth and Atmospheric Sciences, Purdue University, West Lafayette, Indiana
CORRESPONDING AUTHOR: Mallie Toth, Department of Earth and Atmospheric Sciences, Purdue University, 550 Stadium Mall Dr., West Lafayette, IN 47907
E-mail: toth2@purdue.edu

The abstract for this article can be found in this issue, following the table of contents.
DOI:10.1175/2011BAMS3068.1

In final form 11 March 2011

Fig. 1. DOW7 at the Benton County Wind Farm in Indiana during DROPS (photo credit: Erin Jones).

other phenomena for which finescale resolution observations are desired (Wurman et al. 1997). DOWs have participated in numerous field programs in the United States and abroad since the debut of DOW1 during the Verification of the Origins of Rotation in Tornadoes Experiment (VORTEX) in 1995 (Wurman 2001). Several educational deployments have since been undertaken by the DOWs, some before the DOWs were formally supported by the National Science Foundation (NSF; Richardson et al. 2008). The DOW radars are now NSF Lower Atmospheric Observing Facilities and can be requested from the NSF through an expedited process for educational purposes (see www.eol.ucar.edu/deployment/educational-deployments). A DOW was deployed under this educational program to Purdue University for the DOW Radar Observations at Purdue Study (DROPS) in the fall of 2009. DROPS was a field program led primarily by students and was part of the Department of Earth and Atmospheric Science's Radar Meteorology course. During the field program, graduate students and senior undergraduates broke into teams, prepared daily weather briefings, and made decisions on when and where to deploy the DOW. The students were taught the basics of radar operation in the course and, during the deployment, were responsible for using knowledge they gained in class to determine appropriate scanning strategies for the given weather and location. The authors were part of two teams that deployed the DOW on different days to varying locations in close proximity to the Benton County Wind Farm (Figs. 1, 2), an 87-turbine installation located just northwest of the Purdue University campus in Indiana (Benton County Wind Farm 2008).

This research focuses not only on the observations of wind farms made by the DOW but also on observations made by other regional radars. The closest WSR-88D to the Benton County Wind Farm is in Indianapolis (KIND) at about 105-km range, and, because of its placement, the radar has not been compromised by any of the existing Indiana wind farms. KIND, like all radars in the nationwide WSR-88D network, is a 10-cm-wavelength radar with a ~1° beamwidth. The local Lafayette television station radar (WLFI) operates at 5.4 GHz and has a 5.4° beamwidth (Federal Communications Commission 2011), obviously much larger than that of the DOW or the WSR-88Ds. This difference plays a significant role in the amount of wind farm interference observed by the radars.

The amount of interference also depends on the height of the radar beams relative to the turbines. The height of beams above the ground increases with radar range due to the nonzero elevation angles of the radar scans and the curvature of Earth. Under typical operating conditions (i.e., a standard atmosphere in the absence of significant surrounding terrain changes), for example, a target 105 km away from a WSR-88D, the approximate distance from Indianapolis to the Benton County Wind Farm would

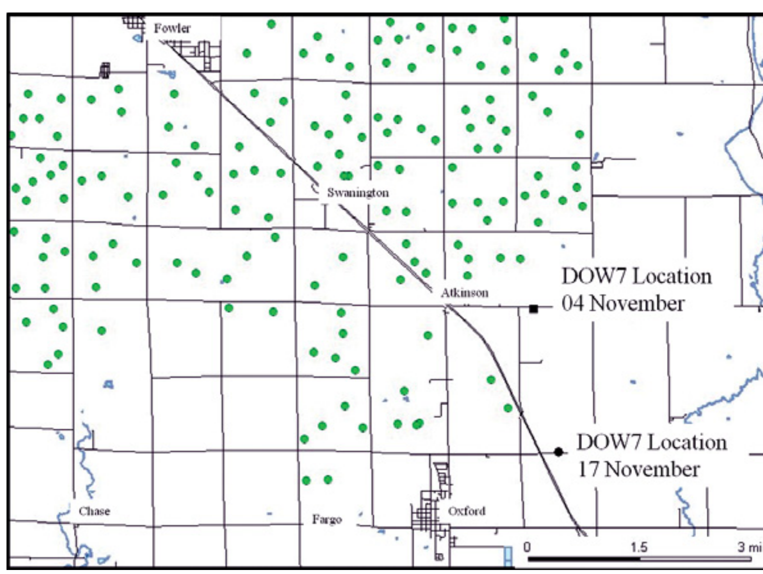

Fig. 2. Map detailing the deployment location of DOW7 with respect to the turbines (represented by the green circles) (map source: Indiana Geological Survey 2011).

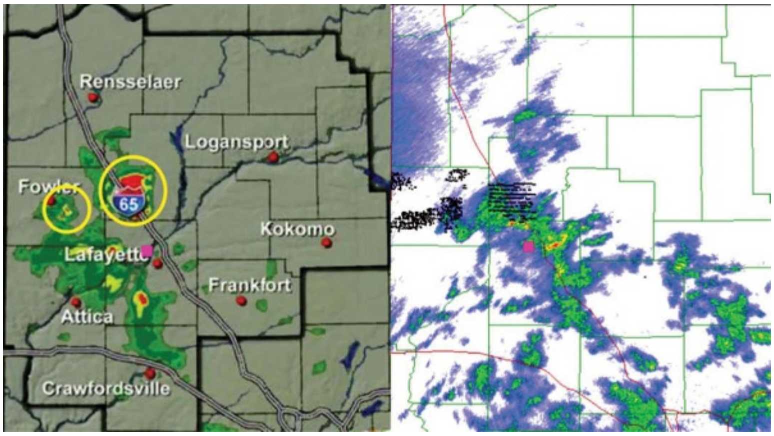

Fig. 3. Radar images from WLFI and KIND. The approximate location of the WLFI radar is denoted by the pink square. Although KIND overshoots the wind turbines [(right) shown by black dots] and samples precipitation returns, WLFI has enhanced reflectivity signatures from the two local wind farms (circled in yellow) (source: WLFI 2011).

be sampled at approximately 1500 m AGL by the center of a beam at a 0.5° elevation angle, well above the height of the wind turbines (see Rinehart 2004). A target closer to the radar, 15 km, for instance, would be sampled at a 0.5° elevation angle at approximately 150 m AGL. With the maximum heights of wind turbines being, on average, between 100 and 150 m above ground level, interference with a radar operating with a 1° beamwidth will most likely occur when turbines are within 15 km of a radar location (Benton County Wind Farm 2008). Furthermore, with increasing distance the beam spreads and samples a larger volume of space; although here we have provided height estimates for the center of the beam at certain distances from the radar, it is the entire sample volume that impacts the power returned to the radar. The Benton County wind turbines reach a maximum height of 118 m with one blade pointing upward. As mentioned previously, the KIND radar easily overshoots the wind farm from more than 100 km away, but the WLFI radar with its 5.4° beamwidth is located approximately 40 km away from the wind farm site, thereby enabling the wind farm to create interference (see examples in Fig. 3). The DOW, at a much closer range to the wind farm, samples the wind turbines quite easily. These relationships are more clearly detailed in Fig. 4.

FIELD EXPERIMENT AND DATA. DOW7 was deployed by two different student groups in close proximity to the Benton County Wind Farm during DROPS: once on a clear-air day and once during heavy precipitation and high winds.

First deployment. The first DOW deployment of interest was on 4 November 2009, a day with scattered clouds and temperatures around 13°C at the time of the deployment (1743–1806 UTC) (Table 1). The nearby Wolcott wind profiler recorded southerly–southwesterly winds of ~5–10 m s^{-1} from the surface to 1 km during this period (Fig. 5). Accordingly, many of the wind turbines were facing south or southwestward. Clear-air plan position indicator (PPI) and range height indicator (RHI) scans were conducted at close range (~0.5 km to the nearest turbine) with a pulse repetition frequency (PRF) of 2500 Hz (Nyquist velocity of ±19 m s^{-1}; Table 2).

The data collected on day 1 resulted in unusual patterns of reflectivity and velocity (Fig. 6). In addition to a high reflectivity return (~50 dBZ) from the wind turbines, streaks in reflectivity, velocity, and spectrum width extending along the radial behind some turbines were noticed. Such patterns appeared in scans only up to ~4.5° in elevation; regions of high

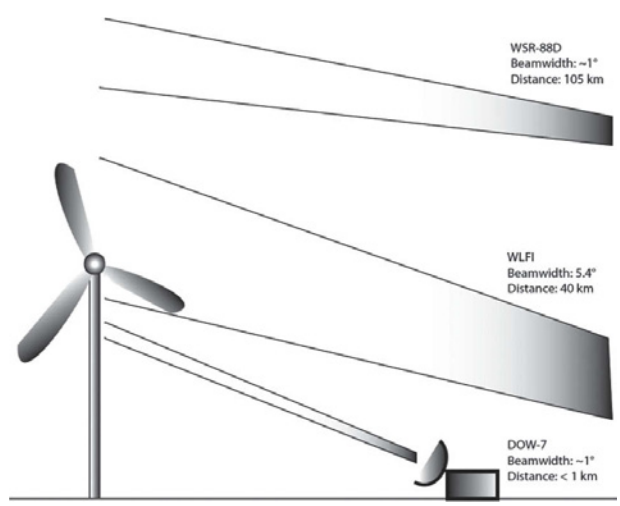

Fig. 4. Diagram (not to scale) detailing how the distance to the wind farms and the beamwidth of the WSR-88D, WLFI, and DOW7 radars impact how much wind turbine interference is observed. The center of the KIND beam is around 1.5 km AGL upon reaching the Benton County Wind Farm; DOW7 samples the individual turbines at various levels depending on their location relative to the DOW. Depending on the scanning strategy of the WLFI radar, the wind turbines will be sampled at various levels.

Table 1. Roof observations on the four-story civil engineering building at Purdue University during both deployments.

	4 Nov 2009	17 Nov 2009
Time of observation (UTC)	1750–1810	1500–1600
Max temperature	12.6°C	6.1°C
Min wind speed (kts)	16	17
Prevailing wind direction	210°	60°

reflectivity then appeared sporadically at 5° and above. Spectrum width was also high in regions of clear air but was much lower in the streaks behind the turbines. In the Doppler velocity fields, azimuthal velocity differences (ΔV) across adjacent beams of as high as 30 m s^{-1} gate to gate were present in the streaks behind the turbines. Because such segments of azimuthal shear occurred along extensive radials, however, they did not have the signature of an isolated vortex (e.g., see Stumpf et al. 1998; Mitchell et al. 1998). Nor did the Doppler velocity returns from the field of wind turbines exhibit random behavior, likely because the operational wind turbines were largely oriented at the same angle with respect to the mean wind. It would therefore be reasonable to infer that the Doppler velocity returns from a field of similarly oriented rotating turbines would follow a predictable pattern, as was observed; radial couplets of outbound and inbound velocities changed in intensity and orientation as the angle of the radar beam changed with respect to the orientation of the turbines. This occurs because, excepting cases in which the turbines are directly facing the radar, the rotating blades would display motion both toward and away from the receiver.

WSR-88Ds have experienced similar interference on a larger scale. Multipath scattering has resulted in spikes of reflectivity beyond the location of the turbines; however, because of scaling, range, and beamwidth with respect to the target, these extensions along a radial are not as apparent in WSR-88D data as they are in the provided DOW examples. Wind turbine interference in reflectivity measurements thereafter impacts velocity measurements and derived products. KIND does not experience these interference effects because of its great distance from the Benton County Wind Farm. Although the WLFI radar is affected by the Benton County Wind Farm, it has not experienced similar multipath scattering issues in clear-air or precipitation scans, possibly because of its large beamwidth. The volume being sampled is so large compared to the turbines that any anomalous returns from the turbines are averaged into a single return of high reflectivity without any defining spikes, as is typically seen by the WLFI radar on clear-air days (Fig. 3).

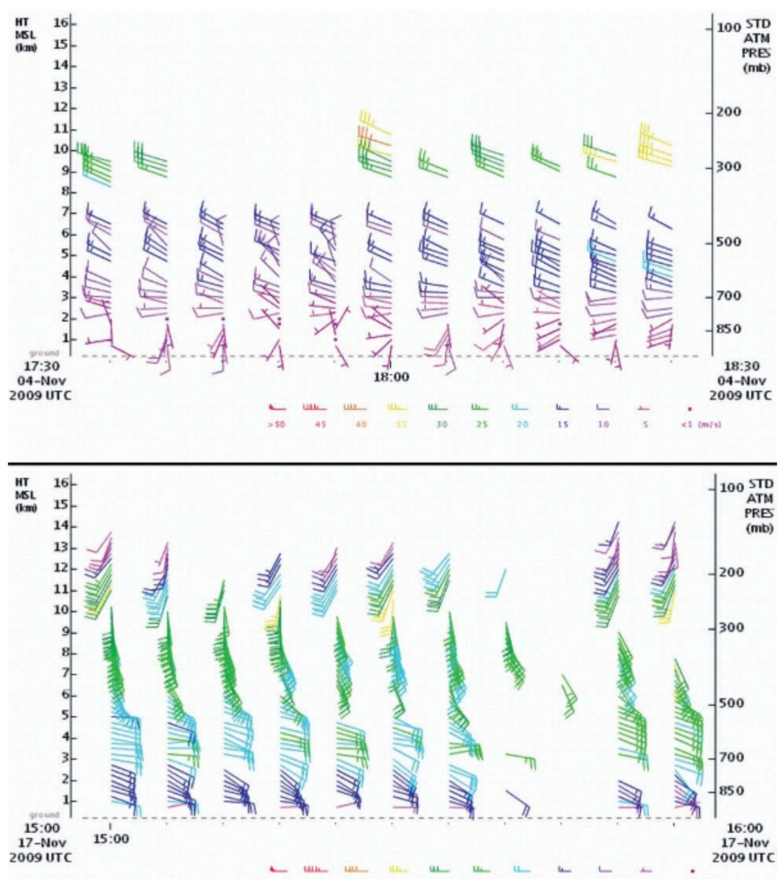

Fig. 5. Vertical wind profiles from the nearby Wolcott, Indiana, wind profiler for both deployment days (source: National Oceanic and Atmospheric Administration 2010).

Table 2. Scanning strategies for 4 Nov 2009 at 40.562°N, 87.224°W.			
Scan type	**Elevation range**	**Azimuth range**	**Azimuth/elevation rate**
PPI	0.5°–15.5°	45°–135°	5° s^{-1}
RHI	0.5°–15.5°	60°–90°	5° s^{-1}
RHI	0.5°–15.5°	90°–120°	5° s^{-1}
PPI	0.5°–15.5°	10°–180°	5° s^{-1}

Second deployment. The second deployment of the DOW at the wind farm was on 17 November 2009, the day with the most extensive and intense precipitation in the entire DROPS field study. This deployment was slightly south of the 4 November location (see Tables 2, 3). The temperature remained around 6°C throughout the deployment (~1500–1600 UTC; see Table 1). Winds recorded at the Wolcott wind profiler (outside the precipitating area during most of the deployment) were easterly at ~5–20 m s^{-1} up to 1 km in altitude during the period (Fig. 5). PPI and RHI scans were conducted with a 2500-Hz PRF (Nyquist velocity of ±19 m s^{-1}; Table 3). The data recorded during the precipitating deployment contain no streaks along a radial; the wind turbines, however, could still be distinguished. High reflectivity returns (~50 dBZ) and strong azimuthal velocity differences (ΔV ~ 30 m s^{-1}) were present in scans up to 1.5° elevation, above which no further evidence of the wind farm was apparent (Fig. 7). Although the second deployment site was not as close to the wind turbines as the clear-air deployment site, evidence of the wind farm was expected in scans above 1.5° in elevation. It is likely that precipitation scatterers overwhelmed the return from the turbines in these conditions.

DISCUSSION. The patterns in the reflectivity and velocity fields observed on the clear-air day (4 November) may be attributed to multipath scattering, a result consistent with the spurious reflectivity observed by multiple WSR-88D facilities (KDDC, KTFX, and KTYX). Because of the proximity of the DOW to the wind turbines, it is reasonable to expect high power returns. There is a notable difference between the patterns observed in all three moments on the clear-air day and the precipitating day. One potential explanation for these differences is changes in the wind turbine blades' "angle of attack," or the angle at which the individual blades are tilted in the vertical with respect to the mean wind flow to generate optimal lift. It should be noted that, for the purpose of this discussion, the angle of attack is not an idea of meteorological origin but is instead a concept of fluid dynamics that may be used by wind energy corporations to maximize the energy generated from wind farms given specific wind conditions (Lanzafame and Messina 2009). For wind turbine blades, the optimal range of the angle of attack that provides the highest turbine speed is 10°–15° relative to the wind direction (Tonch 2003). The standard angle of attack is 4° for the most efficient wind-to-energy conversion. It is possible that during the 4 November scans the turbine blades' angle of attack, determined by the south-southwest wind direction, caused the turbine blades to be oriented in such a way that their vertical tilt, with respect to the radar beam, increased the

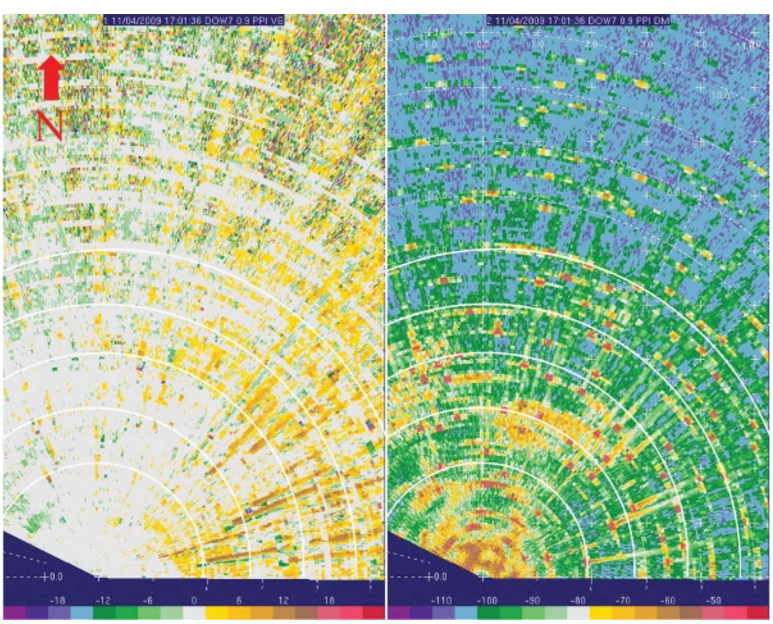

Fig. 6. (left) DOW7 0.5° elevation velocity and (right) reflectivity scans on the clear-air day, 4 Nov 2009. Range rings are at 1-km spacing. Note the presence of the wind turbines at the highest power returned values.

Table 3. Scanning strategies for 17 Nov 2009 at 40.534°N, 87.217°W.			
Scan type	**Elevation range**	**Azimuth range**	**Azimuth/elevation rate**
PPI	0.5°–10.5° (0.5° steps)	360°	30° s^{-1}
RHI	0.5°–10.5° (0.5° steps)	90°–270° (10° steps)	5° s^{-1}
RHI	0.5°–30.5°	90°–270° (10° steps)	5° s^{-1}

amount of power returned and therefore caused high spikes in the reflectivity and velocity fields. This type of blade orientation-dependent interference was also noted by Isom et al. (2009).

The precipitating day (17 November) observations differed from the clear-air day observations in that multipath scattering was not present. In addition to the position of the DOW with respect to the different angle of attack (which perhaps led to a decrease in the blades' radar cross section), the presence of heavy rainfall understandably resulted primarily in observations of precipitation targets because the radar cross section of precipitation targets would have dwarfed that of the turbine blades. The DOW data confirm that wind farms can cause velocity couplets and anomalously high reflectivity values in precipitation. Although the high reflectivity values are not unexpected when the DOW or any weather radar samples a large, solid target, the velocity couplets are reason for concern. Deployment data show the couplets do not extend above the base radar scan, which may result in the base couplet being flagged but may not enact the detection algorithm. A WSR-88D, however, located within its optimal range (~15 km) from the wind farm may detect the turbines and, under certain conditions, activate the detection algorithms. The WLFI radar detects the wind farm in both clear-air and precipitating conditions; this is partly due to the wide beam of the radar and its distance to the site. It is reasonable to assume that the WLFI radar samples a sizeable vertical and horizontal portion of the wind farm as its sample volume increases with range. The averaged sample volume, which includes reflectivity and velocity values from the turbines, appears as if it has sampled a storm with high reflectivity values in the region of the wind farm, regardless of whether precipitation is in the area. WTC is likely already posing problems to other local television stations across the country with similar Doppler radars, although the full extent of the problem is still unknown.

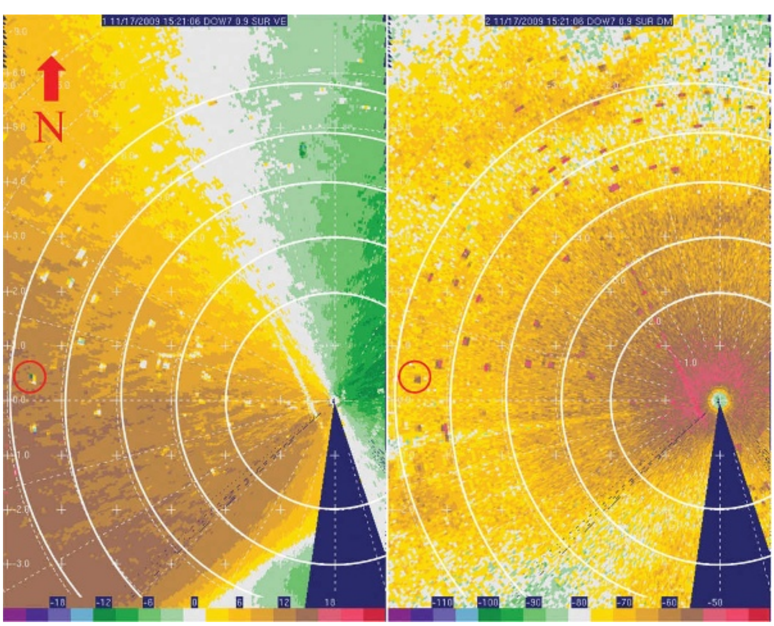

Fig. 7. (left) DOW7 0.5° elevation velocity and (right) reflectivity scans on the precipitating day, 17 Nov 2009. The location of the ~30 m s^{-1} ΔV is circled; this turbine is approximately 5.5 km from the radar. Range rings are at 1-km spacings.

CONCLUSIONS AND FUTURE WORK. The deployment of the DOW near the Benton County Wind Farm in November 2009 resulted in the observation of features that have been found in previous studies on the impact of wind farms on WSR-88D operations, including multipath scattering and velocity couplets that appear as isolated tornadic vortices. The clear-air day exhibited mostly multipath scattering, whereas the main observations on the precipitating day were of isolated velocity couplets. In the DOW data, the features are exaggerated, because of the close proximity of the DOW relative to the wind farms. The data also suggested that the radar return from the turbines, especially in the case of velocity returns, may be affected by the wind direction and the turbine blades' angle of attack, which impacts the orientation of the turbine blades with respect to the radar beams. Velocity couplets on the precipitating day (17 November) were only present in the lowest elevation scans, which may result in the identification of a low-level couplet by the WSR-88D detection algorithms.

As large-scale wind farms are still relatively new in the United States, their impacts on the nation's network of Doppler radars and television station radars have yet to be fully understood. Strategies to mitigate the effects that wind farms have on WSR-88D products and detection algorithms are being discussed and developed, but the full range of problems associated with the expansion of wind farms will continue to unfold. Current attempts to remove the signatures of wind turbines from WSR-88D data in particular operations have been fairly successful (Isom et al. 2009), but these mitigation strategies will need to be expanded to better filter out the WTC under various circumstances operationally. The authors expect the data collected during the DROPS field program will be the first of many smaller-scale observations of wind farms made intentionally or by circumstance in the next few years; indeed, operations during the second phase of the VORTEX2 project were hindered by the presence of wind farms at target storm locations, and some of the project's mobile Doppler radar data may contain wind farm artifacts. It is the authors' hope that such observations begin to highlight the need for a better understanding of wind farm impacts on the varying array of Doppler radars and radar networks being used operationally and in research throughout areas of the globe where wind energy is an important power source. The authors also hope that this work serves to illustrate the importance of enabling students at various educational levels in the atmospheric sciences to have the opportunity to participate in field work and to engage in the investigation of current problems in their area of study. Such programs can not only prove to be an excellent learning experience but may also create a foundation upon which further research can be based.

ACKNOWLEDGMENTS. The DOWs are supported by National Science Foundation Grant NSF-ATM-0734001. DROPS was made possible by the National Science Foundation Lower Atmospheric Observing Facilities for National Center for Atmospheric Research Earth Observatory Laboratory Educational Deployments. We would like to express appreciation to the Center for Severe Weather Research, including Josh Wurman for his input on the manuscript and Justin Walker for his time spent assisting with DOW7 during DROPS. Thanks especially to Jeff Trapp for bringing DOW7 to Purdue and providing guidance for the preparation and content of this manuscript. We would like to express our appreciation to Don Burgess for providing his expertise on our results. We'd also like to acknowledge our other team members, Dan Sheehan and Brenton Kramer, as well as Ernie Agee for his interest in this project.

REFERENCES

Benton County Wind Farm, 2008: Self-guided driving tour of Indiana's first wind farm. Pamphlet, 1 pp. [Available online at www.earlparkindiana.com/windtour/TourPage1.jpg.]

Brotzge, J. A., K. Droegemeier, and D. J. McLaughlin, 2006: Collaborative Adaptive Sensing of the Atmosphere (CASA): New radar system for improving analysis and forecasting of surface weather conditions. *Transp. Res. Rec.,* **1948,** 145–151.

Burgess, D. W., T. D. Crum, and R. J. Vogt, 2007: Impacts of wind turbine farms on WSR-88D radars. Preprints, *33rd Int. Conf. on Radar Meteorology,* Cairns, QLD, Australia, Amer. Meteor. Soc., 13B.6. [Available online at http://ams.confex.com/ams/33Radar/techprogram/paper_123311.htm.]

Crum, T., 2010: Wind farms and the WSR-88D: An update. *Nexrad Now,* **19,** 17–22.

——, and R. L. Alberty, 1993: The WSR-88D and the WSR-88D operational support facility. *Bull. Amer. Meteor. Soc.,* **74,** 1669–1687.

——, E. Ciardi, and J. Sandifer, 2008: Wind farms: Coming soon to a WSR-88D near you. *Nexrad Now,* **18,** 1–7.

Federal Communications Commission, cited 2011: Wireless Telecommunications Bureau universal licensing system. [Available online at http://wireless.fcc.gov/uls.]

Hood, K., S. Torres, and R. Palmer, 2010: Automatic detection of wind turbine clutter for weather radars. *J. Atmos. Oceanic Technol.,* **27,** 1868–1880.

Indiana Geological Survey, cited 2011: IndianaMap. [Available online at http://inmap.indiana.edu.]

Isom, B. M., and Coauthors, 2009: Detailed observations of wind turbine clutter with scanning weather radars. *J. Atmos. Oceanic Technol.,* **26,** 894–910.

Lanzafame, R., and M. Messina, 2009: Optimal wind turbine design to maximize energy production. *Proc. Inst. Mech. Eng.,* **223A,** 93–101.

McLaughlin, D., and Coauthors, 2009: Short-wavelength technology and the potential for distributed networks of small radar systems. *Bull. Amer. Meteor. Soc.,* **90,** 1797–1817.

Mitchell, E. D., S. V. Vasiloff, G. J. Stumpf, A. Witt, M. D. Eilts, J. T. Johnson, and K. W. Thomas, 1998: The National Severe Storms Laboratory tornado detection algorithm. *Wea. Forecasting,* **13,** 352–366.

National Oceanic and Atmospheric Administration, cited 2010: NPN profiler. [Available online at www.profiler.noaa.gov/npn/profiler.jsp.]

Perry, J., and A. Biss, 2007: Wind farm clutter mitigation in air surveillance radar. *IEEE Aerosp. Electron. Syst. Mag.,* **22,** 35–40.

Richardson, Y., P. Markowski, J. Verlinde, and J. Wurman, 2008: Integrating classroom learning and research: The Pennsylvania Area Mobile Radar Experiment (PAMREX). *Bull. Amer. Meteor. Soc.,* **89,** 1097–1101.

Rinehart, R. E., 2004: *Radar for Meteorologists.* Rinehart, 482 pp.

Stumpf, G. J., A. Witt, E. D. Mitchell, P. L. Spencer, J. T. Johnson, M. D. Eilts, K. W. Thomas, and D. W. Burgess, 1998: The National Severe Storms Laboratory mesocyclone detection algorithm for the WSR-88D. *Wea. Forecasting,* **13,** 304–326.

Tonch, F., cited 2003: The blade designer program—A free basic help tutorial in blade design. [Available online at www.windstuffnow.com/main/blade_design_help.htm.]

U.S. Department of Energy, 2008: 20% wind energy by 2030: Increasing wind energy's contribution to U.S. electrical supply. U.S. Department of Energy Rep., 248 pp. [Available online at www.20percentwind.org/20percent_wind_energy_report_revOct08.pdf.]

Vogt, R. J., and Coauthors, 2007: Weather radars and wind farms—Working together for mutual benefit. *Extended Abstracts, WIND-POWER 2007 Conf. and Exhibition,* Los Angeles, CA, AWEA, 1–7.

WLFI, cited 2011: Radar center. [Available online at www.wlfi.com/subindex/weather/radar_center.]

Wurman, J., 2001: The DOW mobile multiple-Doppler network. Preprints, *30th Int. Conf. on Radar Meteorology,* Munich, Germany, Amer. Meteor. Soc., 95–97.

——, J. M. Straka, E. N. Rasmussen, M. Randall, and A. Zahrai, 1997: Design and deployment of a portable, pencil-beam, pulsed, 3-cm Doppler radar. *J. Atmos. Oceanic. Technol.,* **14,** 1502–1512.